

1 **Temporal modulation of the NF-κB RelA 2 network in response to different types of DNA 3 damage**

4 *Amy Campbell^{1†}, Catarina Ferraz Franco^{1†}, Ling-I Su², Simon Perkins³, Andrew R.
5 Jones³, Philip J. Brownridge¹, Neil D. Perkins², Claire E. Eyers^{1*}*

6 ¹Centre for Proteome Research, Department of Biochemistry & Systems Biology, Institute of
7 Institute of Systems, Molecular & Integrative Biology, University of Liverpool, Liverpool, L69
8 7ZB, UK

9 ²Faculty of Medical Sciences, Biosciences Institute, Newcastle University, Newcastle Upon
10 Tyne, NE2 4HH, UK

11 ³Department of Biochemistry & Systems Biology, Institute of Institute of Systems, Molecular
12 & Integrative Biology, University of Liverpool, Liverpool, L69 7ZB, UK

13

14 [†]These authors contributed equally to this manuscript

15 * Correspondence to ceyers@liverpool.ac.uk

1 **ABSTRACT**

2 Different types of DNA damage can initiate phosphorylation-mediated signalling cascades that
3 result in stimulus specific pro- or anti-apoptotic cellular responses. Amongst its many roles,
4 the NF- κ B transcription factor RelA is central to these DNA damage response pathways.
5 However, we still lack understanding of the co-ordinated signalling mechanisms that permit
6 different DNA damaging agents to induce distinct cellular outcomes through RelA. Here, we
7 use label-free quantitative phosphoproteomics to examine the temporal effects of exposure of
8 U2OS cells to either etoposide (ETO) or hydroxyurea (HU) by monitoring the phosphorylation
9 status of RelA and its protein binding partners. Although few stimulus-specific differences were
10 identified in the constituents of phosphorylated RelA interactome after exposure to these DNA
11 damaging agents, we observed subtle, but significant, changes in their phosphorylation states,
12 as a function of both type and duration of treatment. The DNA double strand break (DSB)-
13 inducing ETO invoked more rapid, sustained responses than HU, with regulated targets
14 primarily involved in transcription, cell division and canonical DSB repair. Kinase substrate
15 prediction of ETO-regulated phosphosites suggest abrogation of CDK1 and ERK1 signalling,
16 in addition to the known induction of ATM/ATR. In contrast, HU-induced replicative stress
17 mediated temporally dynamic regulation, with phosphorylated RelA binding partners having
18 roles in rRNA/mRNA processing and translational initiation, many of which contained a 14-3-
19 3 ϵ binding motif, and were putative substrates of the dual specificity kinase CLK1. Our data
20 thus point to differential regulation of key cellular processes and the involvement of distinct
21 signalling pathways in modulating DNA damage-specific functions of RelA.

22

23 **Short title:** DNA damage regulation of the RelA signalling network

24

25 **Abbreviations:** ATM: ataxia telangiectasia mutated; CDK: cyclin-dependent kinase; DMSO:
26 dimethyl sulfoxide; DSB: DNA double stranded breaks; ERK: Extracellular signal-regulated
27 kinase; ETO: etoposide; HU: hydroxyurea; IR: ionising radiation; MS: mass spectrometry;
28 MS/MS: tandem mass spectrometry; PTM: post-translational modifications; UV: ultraviolet

29

30 **Keywords:** DNA damage; RelA; p65; NF- κ B; phosphorylation; Mass Spectrometry,
31 phosphoproteomics; etoposide; hydroxyurea

32

1 INTRODUCTION

2 RelA, also known as p65, is a key member of the NF- κ B family of transcription factors, which
3 serve as 'master regulators' of the cellular inflammatory and stress responses, and are key
4 components that maintain tissue homeostasis and contribute to aging. As part of a functional
5 homo- or hetero-dimer (preferentially with p50), RelA regulates a diverse set of genes involved
6 in core cellular processes such as inflammation, proliferation, apoptosis and metastasis [1].
7 The precise functional roles (the complement of genes transcribed) of RelA are governed both
8 by its post-translational modification (PTM) status, and the transcriptional complexes formed,
9 which are themselves regulated in a co-ordinated fashion through numerous cell signalling
10 pathways [2–4]. PTMs have the potential to regulate many aspects of NF- κ B signalling in
11 response to different stimuli, including nuclear translocation, protein-protein or protein-DNA
12 interactions, and stability, often working in a combinatorial fashion to regulate complex
13 formation and transcriptional output.

14

15 While NF- κ B signalling is commonly associated with inflammation and the immune response,
16 these pathways also play key roles in the cellular response to DNA stress. Consequently,
17 aberrant NF- κ B signalling is observed in, and often a contributing factor to, many human
18 diseases, including autoimmune disorders, chronic inflammatory diseases, and cancer [1,5–
19 7]. NF- κ B signalling is also central to age-related degenerative diseases as a result of
20 accumulated age-related DNA damage [8]. The pro-survival effects mediated by NF- κ B in
21 response to specific-types of DNA damage in part explains the cellular resistance to
22 chemotherapy. Hence, a clear understanding of NF- κ B signalling in response to DNA damage
23 is important, not only in the context of ageing, but also to enhance cancer treatment strategies.

24

25 In response to different types of DNA damage, cells invoke specific responses that promote
26 DNA repair, induce cell cycle arrest, regulate cell death or induce cellular senescence [9,10].
27 For example, inhibition of DNA replication using hydroxyurea (HU), which inhibits ribonuclease
28 diphosphate reductase, arrests cells primarily in S-phase [11–15]. In contrast, agents such as
29 etoposide (ETO), which induces DNA double stranded breaks (DSBs) by preventing
30 topoisomerase II-mediated DNA re-ligation during replication and cell division, cause cells to
31 accumulate in the G2/M phase of the cell cycle [16–19]. Whilst the activation of NF- κ B-
32 responsive genes following DNA stress have been investigated, the mechanisms of regulating
33 these differential outputs remain poorly characterised [1,5–7]. Both HU and ETO invoke a
34 DNA damage stress response through ataxia telangiectasia mutated (ATM)-mediated
35 activation of NF- κ B, leading to elevated levels of NF- κ B targets such as Survivin and Bcl-xL.
36 However, these two types of DNA damaging agents result in distinct cellular responses in a
37 variety of tumor-derived cell lines and in primary cells cancer cells, in part due to induction of
38 different NF- κ B gene expression patterns [19–22]; HU mediates a pro-apoptotic response,

1 while an anti-apoptotic response results following cellular exposure to ETO [22]. Differential
2 involvement of p53 in regulating NF- κ B outputs in response to these different types of DNA
3 damaging agents also plays a role: while the transcriptional response to HU requires p53 for
4 both early and late NF- κ B target gene expression, NF- κ B-mediated transcription in response
5 to ETO is independent of p53 [22].

6

7 The activity of all NF- κ B subunits, including RelA, is extensively controlled by a variety of
8 PTMs including: phosphorylation, acetylation, methylation, glycosylation, proline
9 isomerisation, cysteine oxidation and ubiquitination [23–26]. Of these, phosphorylation
10 accounts for the majority of the well-understood dynamic mechanisms of regulation, both
11 direct e.g. pSer45 modulation of DNA binding [26], and indirect e.g. pSer276, which controls
12 a number of other PTMs, including ubiquitination and thus RelA stability [2,27,28]. Of relevance
13 here, Thr505 phosphorylation has been shown to mediate pro-apoptotic effects upon cisplatin-
14 induced DNA damage [29,30]. Given the complexity of NF- κ B signalling, unravelling the
15 mechanisms by which NF- κ B subunits, particularly RelA, induce differential transcriptional
16 specificity in a context-dependent manner is challenging.

17

18 The sensitivity and versatility of mass spectrometry (MS) makes it ideal for the study
19 (identification and quantification) of dynamic PTMs and the regulated binding partners of
20 transcription factors and their transcriptional complexes. Here we utilise a label free
21 phosphoproteomics approach to map DNA damage-induced changes in RelA binding partners
22 and their phosphorylation status, in response to either HU-induced replicative stress, or ETO-
23 mediated DSB. We find that whilst RelA associated proteins remain largely unchanged as a
24 function of DNA stress, there are notable changes in the dynamics of phosphorylation of the
25 RelA-interactome as a function of treatment. These findings point towards different signalling
26 pathways directing the formation of specific RelA networks dependent on the type of DNA
27 damage that likely help direct transcriptional output and thus the cellular response.

28

29

1 MATERIALS and METHODS

2 Generation and culture of HA-RelA U2OS cells

3 The HA-RelA U2OS cell line was generated by transfecting wild-type U2OS cells with the
4 plasmid pRcRSV HA RelA plasmid, which also expresses the neomycin gene. Cells stably
5 expressing HA tagged RelA were then selected by treatment with G418 (600 µg/mL, Melford
6 Chemicals, cat. no. G0175), with pooled populations of cells used in experiments.

7

8 Cell treatment and lysis

9 U2OS cells expressing HA-RelA were cultured in DMEM supplemented with 10% (v/v) fetal
10 bovine serum, penicillin (100 U/mL), streptomycin (100 U/mL), and L-glutamine (2 mM) at 37
11 °C, 5% CO₂. Once 80% confluence was reached, cells were treated with either 50 µM
12 etoposide (50 mM stock solution in DMSO) or 2 mM hydroxyurea (100 mM stock solution in
13 DMEM, 5% DMSO), by addition to the culture media, for the indicated times. Control cells
14 were grown for the maximum time (2 h) in 0.1% (v/v) DMSO. After removal of the media, cells
15 were washed three times with ice cold PBS and collected in 400 µL of lysis buffer (100 mM
16 Tris-HCl pH 8.0, 150 mM NaCl, 0.5 mM EDTA, 0.5% (v/v) Triton X-100, 0.5% (v/v) NP-40, 1
17 x PhosSTOP™ phosphatase inhibitor cocktail tablet (Roche), 1 x cOmplete™ Protease
18 Inhibitor Cocktail (Roche), 50 U/mL of benzonase) into 1.5 mL microtubes using a cell scraper.
19 Cells were then incubated on ice for 120 min to permit cell lysis to occur. Cell lysates were
20 then cleared by centrifugation (16,000 x g, 10 min, 4°C) and protein concentration was
21 determined using the Bradford assay. A total protein amount of 4 mg was set aside for HA-
22 RelA immunoprecipitation.

23

24 Immunoprecipitation of HA-RelA using Anti-HA magnetic beads

25 Pierce™ Anti-HA Magnetic Beads were washed with 0.05% (v/v) TBST and then with lysis
26 buffer prior to addition of 4 mg cleared cell lysate (at a ratio of beads to protein of 1:2000).
27 Beads and lysate were incubated overnight using an end-over-end rotor at 4°C. Beads were
28 then collected using a magnetic stand and washed three times with 40 mM Tris-HCl pH 8.0,
29 0.1% (v/v) NP-40, 1 mM EGTA, 6 mM EDTA, 6 mM DTT, 0.5 M NaCl, 1 x PhosSTOP™
30 phosphatase inhibitor cocktail tablet (Roche), 1 x cOmplete™ Protease Inhibitor Cocktail
31 (Roche); one time with HPLC grade water and finally, three times with 25 mM ammonium
32 bicarbonate (AMBIC). To recover the immunoprecipitated material, the beads were
33 resuspended in 100 µL of 25 mM AMBIC to which 6 µL of a 1% (w/v) solution of RapiGest
34 (Waters, UK) in 25 mM AMBIC was added. Samples were then heated to 80 °C for 10 min.
35 Supernatants containing the eluted proteins were recovered using a magnetic stand and used
36 for in-solution digestion. For western blots the following antibodies were used: Anti-RelA (SC-
37 372, Santa Cruz), Anti-HA (Merck, HA-7), Anti phospho-histone H2AX (2577, Cell Signalling).

1

2 **In-solution digestion and TiO₂-based enrichment of phosphorylated peptides**

3 Samples were digested with trypsin and subjected to TiO₂-based phosphopeptide enrichment
4 as previously described [31]. In brief, disulfide bonds were reduced by addition of DTT to a
5 final concentration of 4 mM (10 min, 60 °C with gentle agitation). Samples were cooled to
6 room temperature and free cysteines alkylated with 14 mM iodoacetamide (30 min, RT), prior
7 to addition of DTT (to 7 mM final) to quench excess iodoacetamide. Samples were digested
8 with trypsin (1:50 trypsin:protein ratio) overnight at 37°C with light agitation (450 rpm on a
9 Eppendorf thermomixer). Digestion was stopped by the addition of trifluoroacetic acid (TFA) to
10 a final concentration of 0.5% (v/v) and incubated for 45 min at 37°C. RapiGest insoluble
11 hydrolysis products were removed by centrifugation (13 000 x g, 15 min, 4°C). Digested
12 samples were dried by vacuum centrifugation and resolubilized in TiO₂ loading buffer (80%
13 acetonitrile, 5% TFA, 1 M glycolic acid) to achieve a peptide concentration of 1 µg/µL and
14 sonicated for 10 min. TiO₂ beads (50 µg/µL in loading buffer) were mixed at 1400 rpm (with
15 intermittent vortexing to prevent the beads from pelleting) with the resuspended peptides
16 (bead:protein ratio of 5:1) for 20 min at RT. TiO₂ beads were recovered by centrifugation (2000
17 x g, 1 min) and washed successively for 10 min (1400 rpm) with 150 µL of loading buffer, 80%
18 acetonitrile 1% TFA, then 10% acetonitrile, 0.2% TFA. Prior to elution, beads with bound
19 phosphopeptides were dried to completion by vacuum centrifugation. Bound phosphopeptides
20 were then eluted by addition of 100 µL of 1% (v/v) ammonium hydroxide and then with 100 µL
21 of 5% (v/v) ammonium hydroxide. Both elutions were combined and dried by vacuum
22 centrifugation.

23

24 **Liquid chromatography-tandem mass spectrometry (LC-MS/MS) analysis**

25 Phosphopeptide enriched samples were analysed by LC-MS/MS using an Ultimate 3000
26 RSLC™ nano system (Thermo Scientific, Hemel Hempstead) coupled to a QExactive HF
27 mass spectrometer (Thermo Scientific). The samples were loaded onto a trapping column
28 (Thermo Scientific, PepMap100, C18, 300 µm X 5 mm), using partial loop injection, for seven
29 minutes at a flow rate of 4 µL/min with 0.1% (v/v) FA, and resolved on an analytical column
30 (Easy-Spray C18 75 µm x 500 mm 2 µm column) using a gradient of 97% A (0.1% formic
31 acid), 3% B (99.9% ACN 0.1% formic acid) to 60% A, 40% B over 80 minutes at a flow rate
32 of 300 nL/min. Data-dependent acquisition employed a 60,000 resolution full-scan MS scan
33 (MS1) with AGC set to 3e6 ions with a maximum fill time of 100 ms. The 10 most abundant
34 peaks were selected for MS/MS using a 60,000 resolution scan (AGC set to 1e5 ions with a
35 maximum fill time of 100 ms) with an ion selection window of 1.2 m/z and a normalised collision
36 energy of 29. A 20 sec dynamic exclusion window was used to minimise repeated selection
37 of peptides for MS/MS.

38

1 **LC-MS/MS data analysis**

2 LC-MS/MS files were aligned in Progenesis QI for Proteomics label-free analysis software. At
3 this stage, no normalisation was performed and an aggregate file containing raw abundances
4 from all the peaks across all runs was exported from Progenesis. These files were searched
5 against UniProt Human reviewed protein database (downloaded December 2015; 20,187
6 sequences) using MASCOT (v 2.6) within Proteome Discoverer (v. 1.4; Thermo Scientific).
7 Parameters were set as follows: MS1 tolerance of 10 ppm, MS2 mass tolerance of 0.01 Da;
8 enzyme specificity was defined as trypsin with two missed cleavages allowed;
9 Carbamidomethyl Cys was set as a fixed modification; Met oxidation, and Ser/Thr/Tyr/His
10 phosphorylation were defined as variable modifications. Data were filtered to a 1% false
11 discovery rate (FDR) on peptide spectrum matches (PSMs) using automatic decoy searching
12 with MASCOT. *ptmRS* node with Proteome Discoverer was used to determine phosphosite
13 localization confidence. To match *ptmRS* scores to Progenesis MASCOT output files, two
14 rounds of Excel vlookup functions were used: 1) to retrieve scan numbers from the TOP hit
15 per feature number, and 2) to retrieve *ptmRS* score using the corresponding scan number.
16 'Normalizer' software [32] was used to assess the suitability of various types of normalization
17 strategies on the data. Amongst normalization strategies, VSN-G (group-based variance
18 stabilizing normalisation) performed well under various quality control metrics indicating a
19 reduction in technical variance. The 'vsn' R/Bioconductor package [33] was then used to
20 normalize log transformed peptide abundance data for the subsequent stages of analysis.
21 Pairwise t-test and cross condition ANOVA statistical testing, followed by Benjamini-Hochberg
22 global correction was subsequently also performed in R for any replicate groups without
23 missing values. Unless otherwise described, all plots were generated in R.

24

25 **Network analysis**

26 All proteins with quantified phosphopeptides in 2 or more repeats of any condition were
27 combined for network analysis of RelA-associated proteins. Common contaminants that bind
28 non-specifically in IP experiments were removed by filtering protein accessions against a
29 CRAPome database (<https://www.crapome.org>) [34] of contaminants observed with
30 Streptactin-HA IPs from U2OS cells (CC405, CC406 and CC410). All proteins not present in
31 the contaminant database were entered into STRING (<https://string-db.org>, v11.0) to generate
32 a network of protein associations [35]. The generated network was filtered to contain only high
33 confidence associations (interaction score ≥ 0.7) with experimental or database evidence only.
34 Proteins with no high confidence interactions were removed from the network and the
35 remaining nodes were clustered using the Kmeans algorithm (K=9). The resulting network
36 was imported into Cytoscape [36] with nodes recoloured, grouped into the top 9 Kmeans
37 clusters and node shapes for proteins unique to HU or ETO changed to squares or diamonds
38 respectively. For the top 9 Kmeans clusters, nodes corresponding to proteins with differentially

1 regulated phosphopeptides in response to either HU, ETO or both treatments, with respect to
2 the untreated control, were outlined in red, blue or black respectively.
3

4 **Functional enrichment analysis**

5 All functional enrichment analysis was performed using the functional annotation tool in DAVID
6 (<https://david.ncifcrf.gov>, v6.8) against a background of the human proteome [37,38]. For
7 biological process GO term pie charts, all significantly enriched (Benjamini adj.*p*-value ≤ 0.05)
8 GO biological process terms, with associated Benjamini adj.*p*-values, were summarised using
9 REVIGO [39] then visualised with the CirGO Python package [40]. Bubble plots including
10 significantly enriched (Benjamini adj.*p*-value ≤ 0.05) GO biological process (BP), molecular
11 function (MF), cellular component (CC) and overrepresented keywords, filtered to remove
12 duplicate terms, were plotted in R.
13

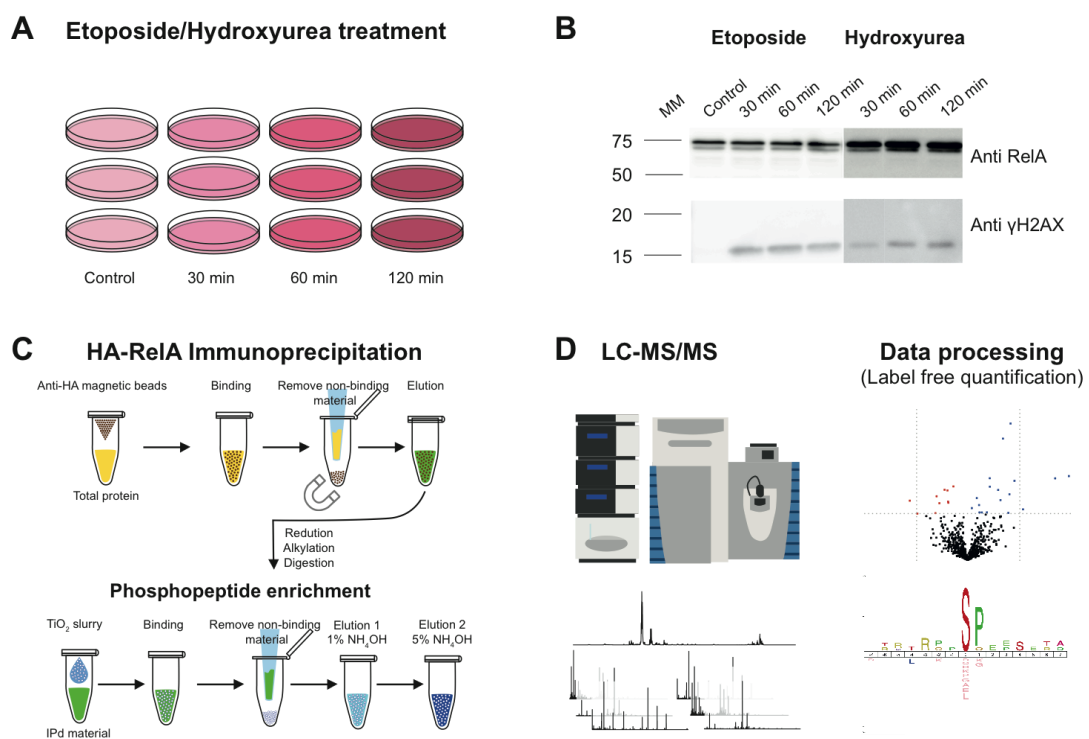
14 **Kinase Prediction/Sequence motif analysis**

15 Kinase-substrate prediction for all differentially regulated (*t*-test, *p* ≤ 0.05) phosphosites was
16 performed using NetPhorest [41,42]. Briefly, for all 'class I' phosphorylation sites (*ptmRS*
17 ≥ 0.75) protein identifiers together with the position of the phosphorylated residue were
18 submitted to NetPhorest using the high-throughput web interface, with the top scoring
19 prediction for each site reported. Kinase predictions were summarised for all up- or down-
20 regulated phosphosites with the resulting data plotted in R. For sequence motif analysis,
21 sequence windows encompassing 7 amino acids either side of the phosphorylated residue
22 were extracted for all phosphosites significantly up- or down- regulated (*t*-test, *p* ≤ 0.05) with
23 respect to the untreated control. Consensus sequence motifs were generated with iceLogo
24 v1.2 [43] against a background of the precompiled human Swiss-Prot composition using
25 percent difference as the scoring system and a *p*-value cut-off of 0.05.
26
27
28

1 RESULTS

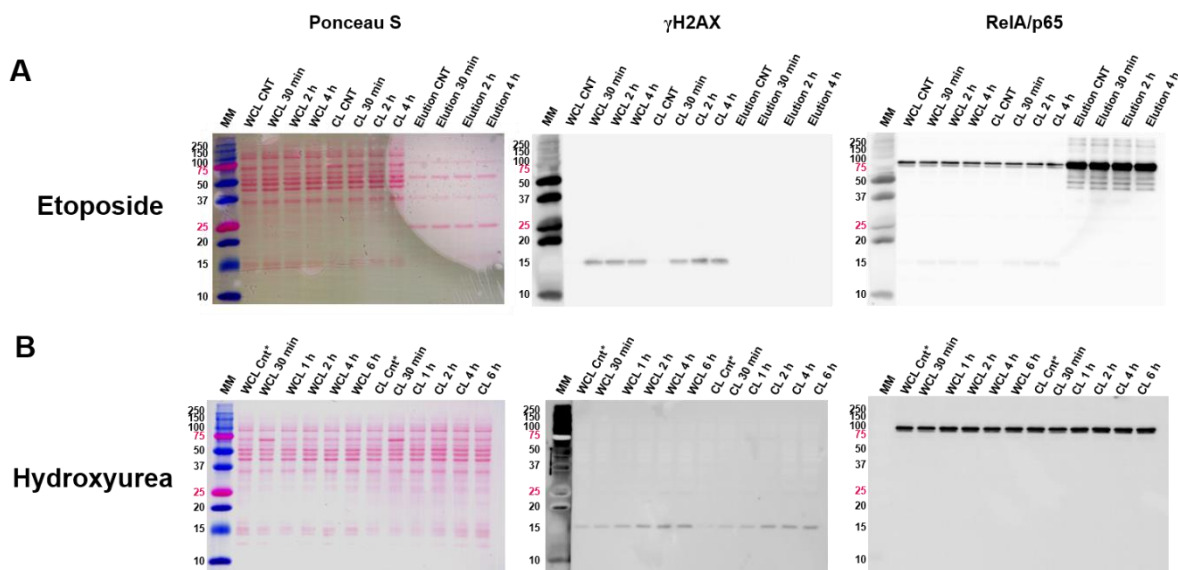
2 Selection of DNA damage timepoints

3 To identify changes in the phosphorylation status of RelA and its protein binding partners in
4 response to different types of DNA damage, we first examined the kinetics of DNA damage
5 after treatment with either the DSB inducer ETO, or the replicative stress inducer HU in the
6 HA-RelA U2OS cell line. Using gamma-H2AX as a marker [44,45], we observed rapid DNA
7 damage (within 30 min) following treatment with either ETO or HU (Fig. 1; Supplementary Fig.
8 1). Gamma-H2AX levels peaked faster with ETO than HU, but sustained (and maximal) levels
9 were observed with both agents following ~ 2 hours of continuous treatment. A time-course of
10 the effect of these different DNA damaging agents on the RelA phosphorylation interactome
11 was therefore evaluated by treatment of the HA-RelA U2OS cells with either ETO or HU for 0,
12 30, 60 or 120 minutes prior to immunoprecipitation (IP) of the HA-tagged RelA.
13 Immunoprecipitated proteins were subject to titanium dioxide (TiO_2)-based phosphopeptide
14 enrichment prior to LC-MS/MS with label-free peptide quantification (Fig. 1).



15
16
17 **Figure 1. Workflow for evaluation of DNA damage response of HA-RelA U2OS cells with**
18 **either Etoposide (ETO) or Hydroxyurea (HU).** (A) HA-RelA U2OS cells were treated with
19 either 0.1% DMSO (control), ETO (50 μM) or HU (2 mM) for the times indicated to induce DNA
20 damage. (B) Following treatment with either ETO or HU, HA-RelA U2OS cell lysates were
21 immunoblotted with antibodies against either γ H2AX as a marker of DNA damage, or
22 RelA/p65. (C) Workflow for evaluation of the phosphorylated RelA interactome. Cells were
23 treated as in (A), and RelA-bound proteins immunoprecipitated with an anti-HA antibody.
24 Proteins were subjected to tryptic digestion and TiO_2 -based phosphopeptide enrichment. (D)
25 Peptides were analysed by LC-MS/MS using a QExactive HF and subjected to label-free
26 quantification following appropriate normalisation.

1



2

3 **Supplementary Figure 1. Time course of treatment of HA-RelA U2OS cells with**
4 **etoposide or hydroxyurea.** HA-RelA U2OS cells were treated for the specified times with
5 either etoposide (A) or hydroxyurea (B) as indicated to assess DNA damage. Cell lysates were
6 separate by SDS-PAGE; total protein was visualised with Ponceau S staining. Gels were then
7 subjected to immunoblotting with antibodies against either γ H2AX as a marker of DNA
8 damage, or RelA/p65. MM: molecular markers; WCL: whole cell lysate; CL: cleared lysate;
9 Elution: eluant from anti-HA beads; CNT: control. Control cells for hydroxyurea treatment were
10 exposed to DMSO for 6 h to match longest treatment time.

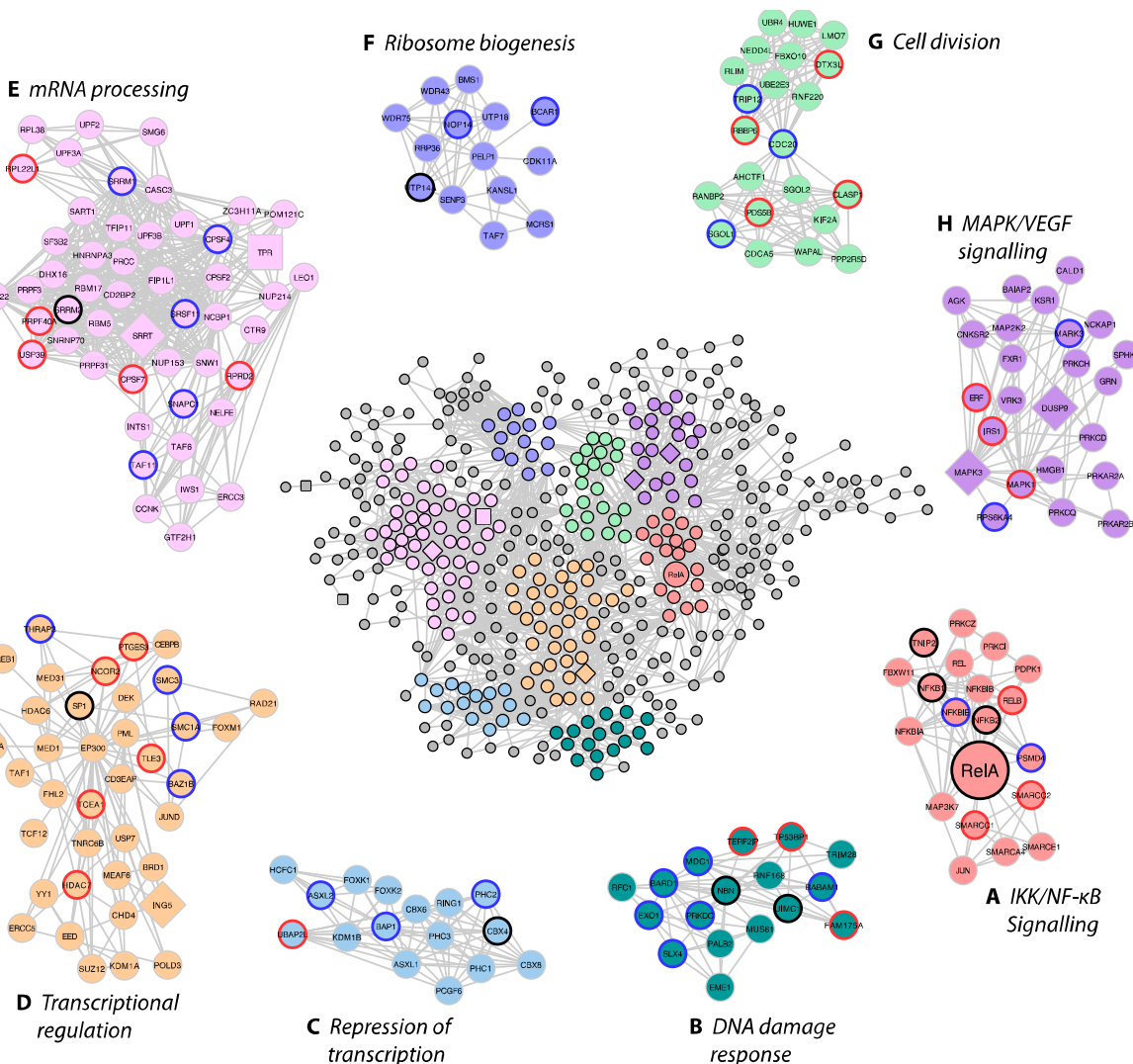
11

12 Network of RelA-associated proteins

13 Using the identified (phospho)peptides as proxy for protein identifications, the list of RelA
14 bound proteins under all conditions was filtered against a 'CRAPome' database of
15 contaminants commonly observed in Streptactin-HA IPs from U2OS cells (CC405, CC406 and
16 CC410), which provided the closest match to the experimental workflow described here.
17 Phosphopeptide quantification data was normalised and subjected to ANOVA testing across
18 all conditions, and individual t-tests across all pairs of conditions. Using this list, the temporal
19 effect of treatment with either ETO or HU on RelA bound phosphoproteins was evaluated for
20 all those proteins quantified in at least 2 biological replicates, under a given condition.

21 To generate a network of high confidence interactors, the remaining 815 RelA-associated
22 proteins combined across all conditions (Supp. Table 1) were inputted into STRING (v11.0)
23 [35] using experimental and database sources only, and clustered using the Kmeans algorithm
24 (k=9). Twelve of these proteins failed to yield high confidence interactions and therefore were
25 filtered out of subsequent datasets (Fig. 2). Gene Ontology (GO) enrichment analysis of
26 biological function for these 803 proteins within the top 9 network clusters confirmed
27 association of RelA with a number of I κ B kinase/NF- κ B signalling proteins (Fig. 2A), including
28 RelB, c-Rel, p105/p50, p100/p52, I κ B α , I κ B β , and the DNA damage response (Fig. 2B).
29 Clusters of proteins across a number of core cellular processes were also identified in the
30 RelA interactome, including key proteins involved in cell division, transcriptional regulation,

1 mRNA/rRNA processing and MAPK/ERK/VEGF signalling (Fig. 2 [A-H]). Amongst these
 2 interactions partners, we also confirmed observation of a number of known RelA binding
 3 proteins, including e.g. replication factor C (RFC1), p300, SP1 and HDAC6 [46–49].



4
 5 **Figure 2. Network map of RelA interacting phosphoproteins.** Proteins from
 6 phosphopeptides quantified following HA-RelA immunoprecipitation in control (0.1% DMSO
 7 control), ETO (50 μ M) or HU (2 mM) treated U2OS cells were evaluated with STRING (v11.0)
 8 [35] for prior experimental evidence of interaction. Kmeans clustering was used to identify the
 9 top 9 enriched GO clusters of biological function and plotted using Cytoscape [36]. The shape
 10 of the nodes represent the conditions under which they were identified: round nodes represent
 11 proteins identified across all conditions; diamond nodes indicate proteins unique to ETO
 12 treatment; square nodes indicate proteins unique to HU treatment. (A) red nodes represent
 13 those proteins mapped to IKK/NF- κ B signalling; (B) dark green nodes represent those proteins
 14 mapped to DNA damage response/DNA repair; (C) blue nodes represent those proteins
 15 mapped to repression of gene expression; (D) yellow nodes represent those proteins mapped
 16 to transcriptional regulation; (E) pink nodes represent those proteins mapped to mRNA
 17 processing/splicing; (F) violet nodes represent those proteins mapped to ribosome
 18 biogenesis/rRNA processing; (G) light green nodes represent those proteins mapped to cell
 19 division/mitosis; (H) purple nodes represent those proteins mapped to MAPK/VEGF signalling.
 20 Proteins outside of these 8 enriched clusters have nodes in grey. The outline colour of the
 21 nodes within the 8 clusters shows proteins with differentially regulated phosphopeptides
 22 following treatment with either ETO (blue), HU (red), or both (black).

1 To determine the temporal response in the RelA interactome of phosphorylated proteins to
2 the different DNA damaging agents, we evaluated those quantified proteins exhibiting a
3 statistically significant (t-test, $p \leq 0.05$) change in response to time-dependent treatment with
4 ETO or HU, in comparison to control (DMSO treated) cells. Interestingly, the constituents of
5 the RelA interactome changed very little in response to DNA damage, with the vast majority
6 of the phosphoproteins identified being observed before and after exposure to either ETO or
7 HU (round nodes, Fig. 2). Of the 803 protein binding partners with high confidence interactors,
8 only 7 were unique to ETO (diamond nodes, Fig. 2; Supp. Table 2), while 8 were specific to
9 HU (square nodes, Fig. 2; Supp. Table 3). Of the 7 ETO-specific proteins identified in this
10 network, 3 are essential components of the ERK/MAPK signalling pathway: the protein
11 kinases ERK1 and PAK, and DUSP9, a dual specificity phosphatase that preferentially targets
12 the MAPK/ERK family. A fourth member of this ETO-specific cohort, AAED1 (which has no
13 known common confident interactors and is therefore not represented in Fig. 2), is also
14 reported to positively regulate the ERK/MAPK (and AKT1) pathway, ultimately leading to
15 upregulation of hypoxia-inducible factor (HIF)-1 α and enhanced glycolysis [50]. In contrast,
16 the 8 HU-specific proteins exhibited diverse biological functions, with only one of these
17 proteins, nucleoprotein TPR, falling into one of the top 8 network clusters (Fig. 2A).

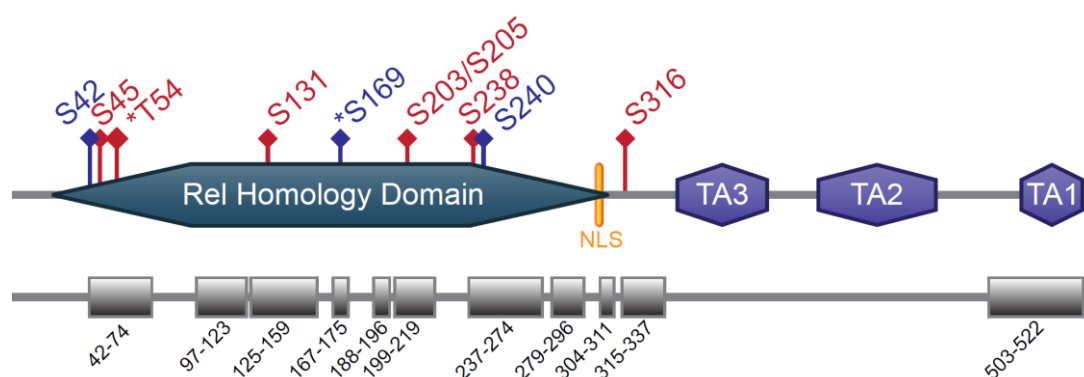
18 Also highlighted in the nodes of the top 8 network clusters are the proteins for which we
19 identified statistically significantly differentially regulated phosphopeptides (t-test, $p \leq 0.05$) in
20 response to treatment with either ETO or HU (or both) with respect to the (DMSO treated)
21 control cells (Fig. 2 [A-H]; Supp. Table 3). Interestingly, the proteins with differentially
22 regulated phosphopeptides following either ETO or HU treatment are largely distinct between
23 the two types of DNA damaging agents, and are interspersed across the network clusters
24 rather than being specific to certain functional biological groups (Supplemental Figure 2-gifs).
25 These data thus suggest that whilst there was relatively little change in the RelA-associated
26 phosphoproteins as a function of DNA damage, the phosphorylation states of those
27 associated proteins was dependent on both the type and duration of the induced DNA damage
28 response.

29

30 **RelA is minimally differentially phosphorylated in U2OS cells in response to ETO or**
31 **HU treatment**

32 Looking specifically at RelA, we observed good sequence coverage of the N-terminal region
33 (>70%; 46% overall; Supp. Fig. 3), allowing us to quantify most of the known phosphorylation
34 sites in the N-terminal half of the protein including; Ser42, Ser45, Ser131, Ser203/Ser205,
35 Ser238, Ser240 and S316. Two novel phosphorylation sites at Thr54 and Ser169 were also
36 observed (Supp. Fig. 3). No phosphorylation sites were confidently identified in the C-terminus
37 of RelA containing the transactivation domains (TAs), in part due to the limited ability to
38 generate suitable tryptic peptides for analysis (as documented previously [26]). Although
39 phosphopeptides covering the extreme C-terminus (from residue 503 and including the known

1 sites of phosphorylation at T505, S529 and S536) were observed, the site of phosphorylation
2 could not be unambiguously defined.
3 Overall, the changes observed in RelA phosphorylation in response to DNA damage under
4 these conditions were very limited. Only Ser131 was statistically significantly regulated by both
5 the DSB-inducing ETO and HU: pSer131 increased marginally by 1.03-fold (with respect to
6 the DMSO-treated control) at 120 min (p -value = 0.047) in response to ETO, responding much
7 more rapidly to HU, increasing 1.05 fold by 30 min (p -value = 0.046), decreasing slightly
8 (although not statistically) by 60 min, and returning to baseline levels by 120 min. We have
9 previously shown that this site is also responsive to TNF α treatment of U2OS cells, and
10 phosphorylated *in vitro* by IKK β , in a manner that is significantly enhanced in the presence of
11 the RelA dimerization partner, p50, and reduced in the presence of I κ B α [26]. In contrast,
12 Ser45, a phosphorylation site that we previously demonstrated plays a critical role in reducing
13 the ability of RelA to bind to DNA (alongside Ser42, which was not observed in the HU-treated
14 cells) [26], was reduced by 1.1 fold (p -value < 0.01) 60 min after cellular treatment with HU,
15 suggesting an HU-mediated regulation of RelA transcription, in part through Ser45
16 phosphorylation (Supp. Fig. 3).



17
18 **Supplementary Figure 3. Schematic of RelA protein coverage.** Domains and quantified
19 sites of phosphorylation are indicated. Blue phosphorylation sites were quantified in ETO only,
20 red were quantified in both ETO and HU. Novel phosphorylation sites are represented with an
21 asterisk. Protein sequence coverage is represented by the boxes (and amino acid residue
22 numbers) in the bottom panel. TA = transactivation domain; NLS – nuclear localisation
23 sequence.
24

25 **ETO and HU induced different phosphorylation dynamics in the RelA network**

26 Of the 696 proteins identified in the RelA network in the presence of ETO, 184 exhibited ETO-
27 dependent changes in phosphorylation status, with a total of 312 phosphopeptides exhibiting
28 a statistically significant change. GO term analysis of biological processes of these 184
29 proteins revealed enrichment primarily of proteins involved in transcription (p < 0.001), RNA
30 processing (p < 0.001), cell division (p < 0.001) and, unsurprisingly, the DNA damage
31 response (p < 0.001) (Fig. 3A). Slightly fewer changes arose in response to HU, with 235
32 phosphopeptides from 157 proteins exhibiting a statistically significantly change compared to
33

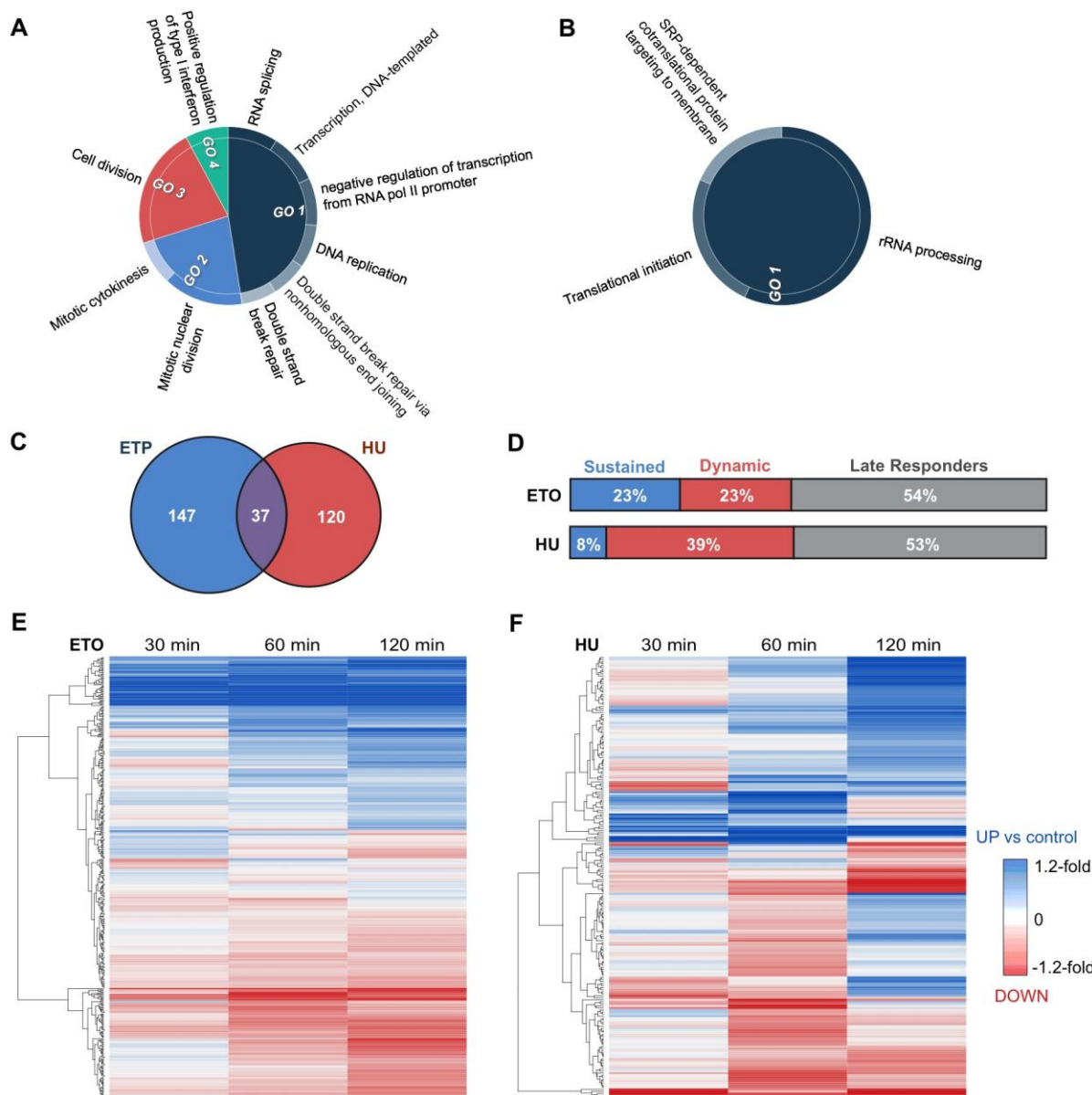


Figure 3. Etoposide and Hydroxyurea induced different phosphorylation dynamics in the RelA network. GO term biological process enrichment was examined for all phosphopeptides exhibiting a statistically significant change in response to either (A) etoposide (ETO) or (B) hydroxyurea (HU). (C) Overlap of those proteins with significant change in phosphopeptide abundance at one or more time points with ETO or HU. (D) Distribution of phosphopeptide changes between sustained, dynamic and late responders for ETO vs HU treatment, where 'Late Responders' indicates a change at 120 minutes only, 'Sustained' indicates a change at 30 or 60 minutes which is sustained throughout, and 'Dynamic' indicates a change at 30 or 60 minutes which is reversed. (E, F) Heatmaps of the fold change in phosphopeptide levels following treatment with either ETO (E) or HU (F) at 30, 60 or 120 min relative to control levels. Hierarchical row clustering was performed on the \log_2 fold changes.

control (Fig. 3B), those primarily being involved in translation ($p < 0.001$) and rRNA processing ($p < 0.001$). Interestingly, only 37 of the proteins exhibiting dynamic changes in response to treatment were common between the two types of DNA damaging agent, indicating significant

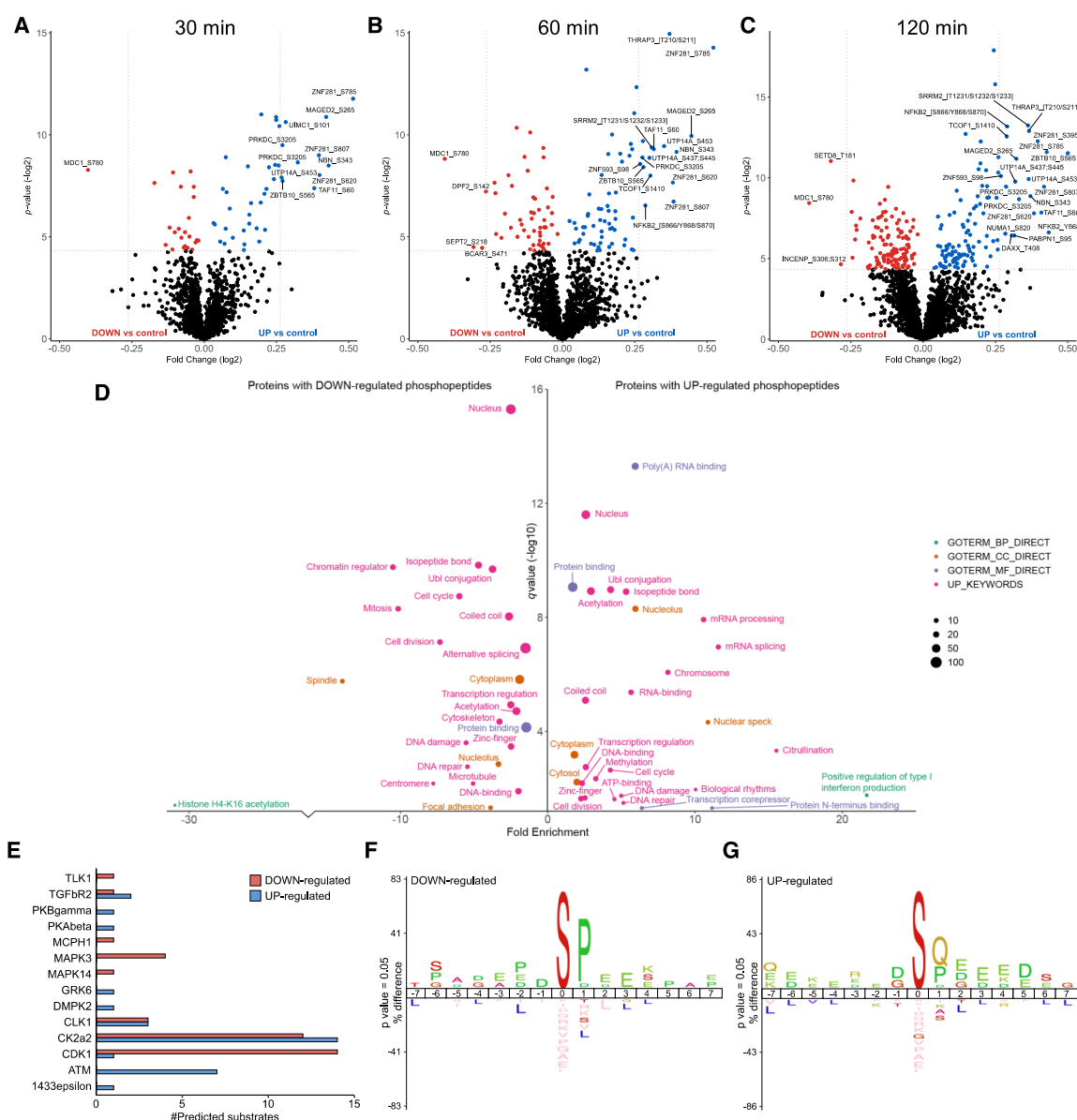
1 differences in the mechanisms whereby RelA mediates the outputs from these two DNA
2 damaging agents (Fig. 3C).
3 We next evaluated the temporal dynamics of these phosphorylation changes as a function of
4 treatment type (Fig. 3D). Intriguingly, ETO and HU induced very different dynamics in
5 phosphosite regulation. Indeed, approximately one-quarter (~70 phosphopeptides) of the
6 ETO-regulated phosphopeptides, were responsive within 60 min of treatment, with the change
7 in phosphorylation status being maintained over the duration of the 120 min experiment (Fig.
8 3D, E). In contrast, only 8% (~20 phosphopeptides) of HU-dependent phosphorylation
9 changes occurred within the first 60 min and were then sustained for the duration (Fig 3D, F).
10 Overall, HU-mediated phosphorylation changes were much more dynamic, with 39% of the
11 phosphopeptides quantified in these experiments significantly regulated (being observed at
12 either increased, or reduced levels), before reverting back, either to control levels, or in some
13 instances, in the opposite direction. Just over half of those phosphopeptides that were
14 differentially regulated by either ETO or HU did not exhibit a statistically significant change
15 until after more than 60 min of continuous treatment, *i.e.* they were late responders that were
16 only observed in these experiments 120 min after exposure (Fig. 3D).
17

18 **Phosphorylation of RelA-associated proteins in response to etoposide**

19 Of the 312 phosphopeptides that were differentially regulated by ETO (with respect to the
20 untreated control ($p \leq 0.05$)) across all time-points, 151 increased in abundance, while 159
21 were down-regulated (Supp. Table 2). Only two phosphorylation sites exhibited significant
22 temporal dynamics (with levels being significantly elevated or decreased at sequential time-
23 points), although the selective nature of the timing at which these measurements were made
24 could be masking additional dynamics. Overall, the relative fold change in phosphopeptide
25 abundance (up- or down-) was relatively small, with the greatest statistically significant fold
26 change being ~1.4 (Fig. 4A-C; Supp Table 2).

27 In-depth functional enrichment analysis of proteins that were either up- or down-regulated
28 following ETO exposure revealed some key differences in terms of the biological functions
29 that were regulated (Fig. 4D). RelA-associated proteins with an ETO-mediated reduction in
30 phosphopeptide levels showed significant enrichment for GO terms including mitosis,
31 chromatin regulation (including H4-K16 acetylation), transcriptional regulation and DNA
32 damage repair (Fig. 4D). pSer780 on MDC1, the Mediator of DNA damage checkpoint protein
33 1, exhibited the greatest down-regulation of all phosphosites in response to ETO across the
34 time-points investigated (1.3-fold down; $p = 1.95E-04$) (Supp. Table 2, Fig. 4A-C). This
35 phosphorylation site has previously been identified as being induced in response to ionising
36 radiation (IR) [51] and ultraviolet (UV) radiation [52], both of which induce DSB, although the
37 physiological function of this phosphorylation site has not yet been defined. We show here
38 that the proportion of Ser780 phosphorylated MDC1 that contributes to the RelA interactome

1 decreases in response to ETO, suggesting that DNA-damage induced pSer780 may serve to
 2 disrupt the interaction of MDC1 with RelA transcriptional complexes.
 3



4 **Figure 4. Etoposide-mediated phosphopeptides changes in the RelA network.** Volcano
 5 plots showing fold changes in phosphopeptide abundance following Bayesian statistical
 6 analysis to evaluate significant differences as a function of (A) 30 min, (B) 60 min or (C) 120
 7 min treatment with ETO. Log₂-fold change are presented as a function of the -Log₂ p-value;
 8 differentially down-regulated (red) or up-regulated (blue) phosphopeptides with a p-value
 9 ≤ 0.05 are highlighted. Select data points are annotated with their protein accession number
 10 and site of phosphorylation. (D) GO term enrichment analysis using DAVID of proteins with
 11 significantly regulated phosphopeptides in response to ETO (all time points) relative to control.
 12 Phosphopeptides with a Benjamini-Hochberg adjusted p-value ≤ 0.05 are labelled. BP =
 13 biological process (green); CC = cellular compartment (yellow); MF = molecular function
 14 (purple); UP = UniProt keyword (pink). (E) NetPhorest kinase-substrate prediction for
 15 significantly down- (red) or up-regulated (blue) phosphosites. IceLogo sequence analysis of
 16 (F) down-regulated or (G) up-regulated phosphosites.

1 It is interesting to note that many more phosphopeptides were significantly upregulated than
2 were decreased in the RelA interactome in response to ETO, particularly in the later time
3 points. Transcriptional regulation and DNA damage repair were also among the GO terms
4 enriched for those proteins with up-regulated phosphorylation sites. However, there was only
5 an ~8% overlap in common proteins with differentially regulated (up or down in response to
6 ETO) phosphopeptides (Supp. Table 2), suggesting co-ordinated regulation of these key
7 processes largely through different protein effectors rather than differential phosphorylation-
8 mediated regulation of the same proteins. Also among the GO terms enriched in the list of
9 proteins with up-regulated phosphopeptides in response to ETO were mRNA processing, ATP
10 binding, transcription corepressor functionality and type I interferon production, including the
11 NF- κ B signalling proteins (RelA (pSer131), NFKB1 (p105/p50) (pSer923;Ser927) and NFKB2
12 (p100/p52) (pSer858, pTyr868 and pSer870), with pSer619 on the RNA helicase DDX41 and
13 pSer3205 on the DNA-dependent protein kinase PRKDC (Fig. 4D). Multiple phosphopeptides
14 from the transcription factor zinc finger protein 281 (ZNF281/GZP1/ZBP99), containing
15 pSer395 ($p = 2.1\text{E-}02$), pSer620 ($p = 1.1\text{E-}04$), pSer785 ($p = 1.9\text{E-}06$) and pSer807 ($p = 1.7\text{E-}03$), were significantly upregulated across all time points (between 1.2-1.4-fold) in the RelA
17 interactome in response to ETO, but not in response to HU. ZNF281 has recently been
18 reported to be recruited to DSBs, following interaction of its zinc finger domain with XXCR4
19 [53], where it plays an important role in non-homologous end-joining upon DNA damage, and
20 consequently the maintenance of cell viability. Supporting our findings of increased
21 phosphorylation in response to DSB, these authors also reported a slight reduction in the
22 recruitment of a non-phosphorylatable S785A/S807A ZNF281 mutant to sites of DNA damage.
23 Based on our data, we would suggest that phosphorylation of ZNF281 on Ser395 and Ser620
24 may also be required for its optimal recruitment to DNA lesions and subsequent DNA repair.
25 In an attempt to understand the signalling pathways and possible kinase-substrate
26 relationships feeding into the ETO-dependent changes in phosphorylation of the RelA-binding
27 partners, the 'class I' localized phosphosites ($ptmRS \geq 0.75$) with p -value ≤ 0.05 were used as
28 input sequences for the NetPhorest kinase-substrate prediction algorithm [34,35] (Fig. 4E). Of
29 the 117 down-regulated and 107 up-regulated phosphorylation sites that passed the above
30 thresholds, NetPhorest gave kinase-substrate predictions for 37 and 32 sites respectively.
31 Among the down-regulated sites, CDK1 had the highest number of predicted substrates (14,
32 38%) which accounts, at least partially, for the notable enrichment across all the ETO down-
33 regulated phosphorylation sites for Pro in the +1 position with respect to the site of
34 phosphorylation [54] (Fig. 4F). The identification of four predicted substrates for ERK1
35 (MAPK3), which is also a Pro-directed protein kinase [55], likely also contributes to the
36 identified sequence motif, and correlates with our observations of this enzyme, and
37 importantly, a cognate phosphatase, DUSP9, in the RelA network under these conditions.

1 IceLogo sequence analysis of the ETO up-regulated phosphosites showed significant
2 enrichment for Gln (and to a lesser extent Pro) at the +1 position with respect to the site of
3 phosphorylation (Fig. 4G). Positions +2 to +5 also exhibited a strong preference for acidic
4 residues (Asp/Glu), consistent with observation of 14 predicted substrates for casein kinase II
5 alpha (CK2α2) in the NetPhorest output (Fig. 4E). Perhaps not surprisingly given its somewhat
6 promiscuous substrate repertoire, and an involvement in diverse cellular processes (including
7 regulation of numerous transcription factors such as NF-κB), CK2α2 was also predicted as
8 the regulatory enzyme for a number of the significantly down-regulated phosphorylation sites.
9 The striking observation of Gln at +1 in 36 of the up-regulated phosphorylation sites (Fig. 4G)
10 is in agreement with previous reports of ATM/ATR-dependent regulation of the RelA NF-κB
11 pathway in response to DSB (albeit following cellular exposure to TNFα rather than etoposide)
12 [56]. ATM/ATR kinases are well known to preferentially phosphorylate Ser/Thr residues
13 following by a Gln, with substrates often containing several closely spaced SQ/TQ motifs in
14 regions termed SQ/TQ cluster domains (SCDs) [57]. Whilst just 7 of the 36 SQ motif-
15 containing sequences were predicted by NetPhorest to be ATM sites, it is possible that many
16 more of the differentially regulated phosphosites that match to this consensus are potential
17 ATM/ATR substrates, given the limitations of prediction software. While phosphorylation at
18 any given site can be induced by more than one protein kinase in cells, the NetPhorest
19 algorithm is best used as a guide and will only assign a single potential enzyme, based on the
20 best fit, and is therefore not fully representative of cellular possibilities.

21 **Phosphorylation of RelA-associated proteins in response to hydroxyurea**

22 Upon HU treatment, 235 phosphopeptides from 157 proteins in the RelA interactome network
23 were significantly differentially regulated with respect to the DMSO treated control ($p \leq 0.05$;
24 Fig. 5 A-C). Of those, 121 phosphopeptides increased in abundance, while levels reduced for
25 109 phosphopeptides. Among the phosphorylation sites exhibiting a dynamic response over
26 the time-course of HU treatment, five showed a bi-directional response, increasing in some
27 time points, but reducing in others, with respect to control levels (Supp. Table 3). RelA-
28 associated proteins with statistically significantly reduced phosphopeptide levels in response
29 to HU-mediated DNA damage were notably enriched for GO terms encompassing ribosome
30 biogenesis, mRNA processing and translation (Fig. 5D). Notably, whilst translation was
31 enriched among the proteins effected by HU treatment there was no significant enrichment for
32 proteins involved in translation with ETO. In contrast, elevated phosphopeptide levels were
33 observed for processes such as chromatin regulation and chromosomal rearrangement, and
34 to a lesser extent, transcriptional regulation and mitosis (Fig. 5D). Whilst transcriptional
35 regulation was among the GO terms enriched in response to HU, it was only marginally
36 enriched, and with a much lower significance than our observations with ETO, suggesting a
37 more limited effect on transcriptional regulation with HU than with ETO (Fig. 4D, Fig.
38 5D).

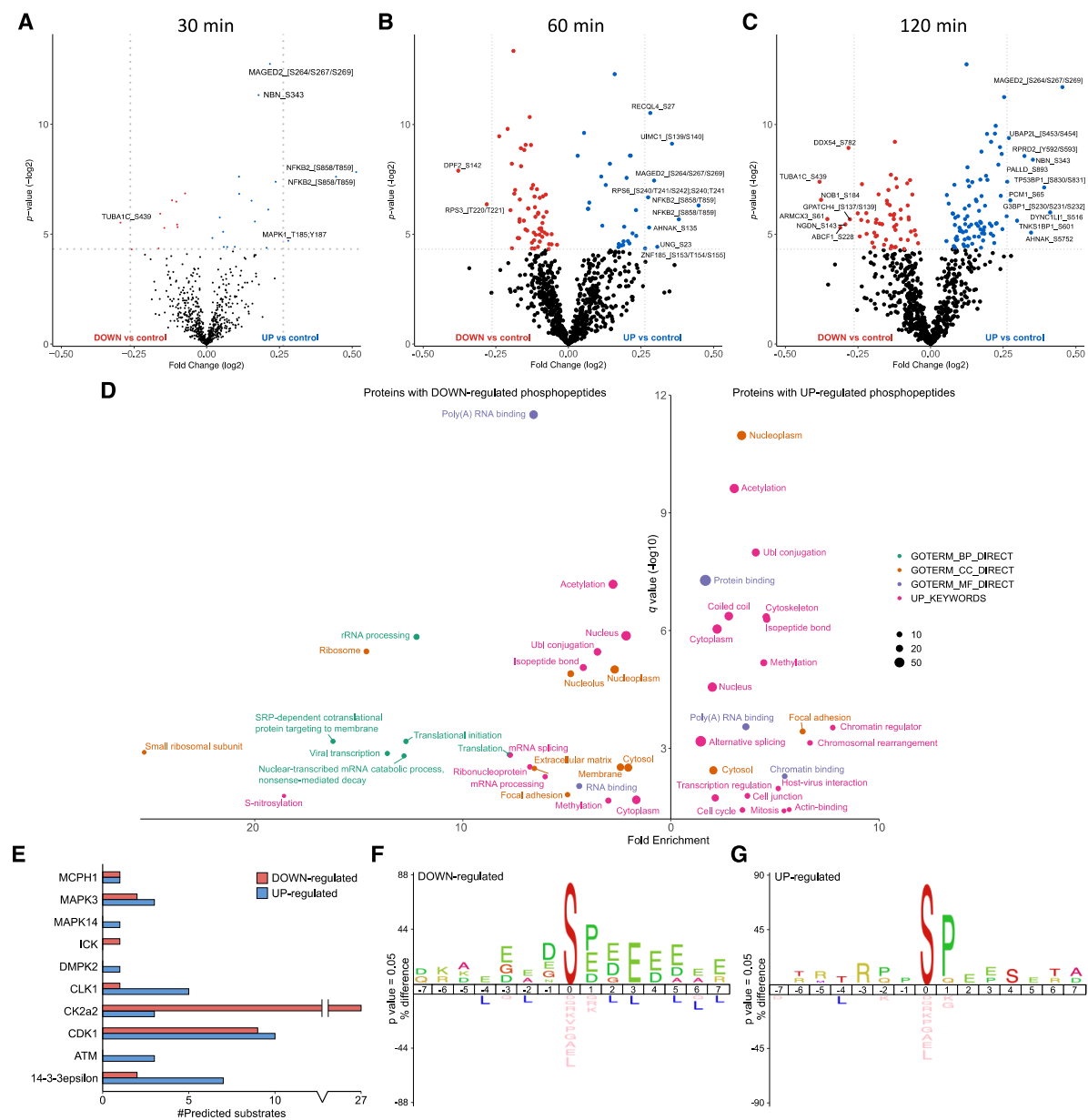


Figure 5. Hydroxyurea-mediated phosphopeptides changes in the RelA network. Volcano plots showing fold changes in phosphopeptide abundance following Bayesian statistical analysis to evaluate significant differences as a function of (A) 30 min, (B) 60 min or (C) 120 min treatment with HU. Log₂ fold change are presented as a function of the -Log₂ p-value; differentially down-regulated (red) or up-regulated (blue) phosphopeptides with a p-value ≤ 0.05 are highlighted. Select data points are annotated with their protein accession number and site of phosphorylation. (D) GO term enrichment analysis using DAVID of proteins with significantly regulated phosphopeptides in response to HU (all time points) relative to control. Phosphopeptides with a Benjamini-Hochberg adjusted p-value ≤ 0.05 are labelled. BP = biological process (green); CC = cellular compartment (yellow); MF = molecular function (purple); UP = UniProt keyword (pink). (E) NetPhorest kinase-substrate prediction for significantly down- (red) or up-regulated (blue) phosphosites. IceLogo sequence analysis of (F) down-regulated or (G) up-regulated phosphosites.

In agreement with the γ H2Ax immunoblotting data (Fig. 1B) which indicated a slower cellular response to HU than ETO (see the heatmaps in Fig. 3F), very few significant changes in phosphopeptide abundance were observed 30 min after treatment with HU (Fig. 5A).

1 Interestingly, the NFKB2 (p100) peptide phosphorylated on either Ser858/Thr859 (site
2 ambiguous) exhibited the greatest increase of any phosphopeptides at this time point, with a
3 1.4-fold change (Supp. Table 3; being observed in two charge states) (Fig. 5B). This increase
4 in HU-mediated phosphorylation is supported by additional quantification of a smaller peptide
5 in which the site of phosphorylation was defined as Ser858 (Supp. Table 3), a site which was
6 also significantly upregulated following exposure to ETO (Supp. Table 2). Of note, these
7 peptides (and others in the C-terminus of p100 that are differentially regulated in response to
8 treatment) are specific to p100, rather than the transcriptionally active p52 cleavage product,
9 suggesting DNA damage-mediated regulation of either p100 processing, or its ability to bind
10 (directly or indirectly) to RelA.

11 The second most differentially elevated phosphopeptide after 30 (and 60) min treatment with
12 HU was the doubly phosphorylated pThr185/pTyr187-containing peptide from ERK2. This
13 phosphopeptide lies in the kinase activation loop and phosphorylation of both of these sites is
14 required for catalytic activation of ERK2 [58,59]. An early consequence of HU treatment on
15 the RelA interactome network thus appears to be activation of bound ERK2, which contrasts
16 with our observations with ETO, where there were no significant changes induced in
17 MAPK1/ERK2 phosphopeptides. Together, these findings are curious in light of the fact that
18 the C-terminal region of p100 is reported to bind to inactive ERK2, thereby preventing its
19 phosphorylation and nuclear translocation. The fact that we observe increased
20 phosphorylation of ERK2 alongside phosphorylation in the C-terminal ‘death domain’ of p100
21 may suggest a role for these p100 phosphorylation sites in regulation its ability to interact with
22 ERK2 [60].

23 Nibrin, a member of the MRN complex which plays a critical role in DSB repair and cell cycle
24 checkpoint control, also exhibited elevated Ser343 phosphorylation by 30 min HU treatment.
25 Interestingly, the pSer343 site observed falls within an SQ motif which has previously been
26 shown to be phosphorylated by ATM in response to IR, and is believed to play a role in intra-
27 S phase checkpoint activation [61,62] (Fig. 5A and 5E). This same phosphorylation site was
28 also rapidly elevated in response to ETO (Fig. 4B), confirming its apparent involvement in a
29 generic ATM-mediated DNA damage response [61,62]. By 60 min, we also observed reduced
30 levels of pSer142 on DPF2 (Zinc finger protein ubi-d4), a known regulator of the non-canonical
31 NF- κ B pathway [63], and pThr220/221 (site ambiguous) on the RelA binding partner RPS3
32 (40S ribosomal protein S3), both of which have previously been reported to be elevated in
33 HEK293 cells following 3 h UV exposure [52]. Although binding of RSP3 to RelA is thought to
34 enhance its ability to bind DNA *in vitro* [64], RSP3 functions as a negative regulator of H₂O₂-
35 mediated DNA repair [65]. It is possible therefore that pThr220/221 on RPS3, and pSer142 on
36 DPF2, serve to modulate the RelA transcriptional complexes and/or the consensus promoter
37 regions for NF- κ B binding, that are required for DNA repair in response to HU.

38

1 Using NetPhorest [41,42], we were able to predict possible kinase-substrate relationships for
2 46% (77 out of 167) of the 'class I' phosphosites ($ptmRS \geq 0.75$) that were regulated in
3 response to HU (Fig. 5E). CK2 α 2 was predicted as the kinase responsible for the vast majority
4 (27 out of 43) of the phosphosites reduced in response to HU, based on the prevalence of
5 acidic residues C-terminal to the site of phosphorylation (in particular at +3) clearly evident in
6 the sequence analysis (Fig. 5F). Consequently, HU might have significant effects on CK2 α 2
7 (or other acidophilic kinases) that feed into the RelA-mediated DNA damage response.
8 Prevalent among both up- and down-regulated phosphosites were predicted substrates of
9 cyclin dependent kinase 1 (CDK1) which, together with the prediction of substrates for ERK1
10 (MAPK3) and p38 α (MAPK14), contributes to the enrichment of Pro at the +1 position in both
11 the HU up- and down-regulated phosphosites (Fig. 5F and 4G). Also among the up-regulated
12 phosphopeptides are a number of predicted ATM substrates which, whilst only representing
13 a small proportion of the total number of HU-regulated phosphosites, corresponds with the
14 small enrichment for Gln in the +1 position among the up-regulated phosphosites. (Fig. 5E
15 and 5G).
16 Comparing the putative kinase-mediated regulation of substrates for those differentially
17 regulated phosphopeptides in the RelA interactome in response to the two different types of
18 DNA damaging agents revealed some interesting observations: although ATM-predicted
19 substrates were enhanced with both ETO and HU, over twice as many putative substrates
20 were elevated with ETO. Predicted substrates for CK2 α 2 are prevalent in the differentially
21 regulated (both up- and down-) phosphosites under both conditions, although HU induces a
22 far greater reduction in levels of putative CK2 α 2 substrates than ETO. In contrast, putative
23 substrates for the dual specificity protein kinase CLK1, which has a role in regulating
24 alternative splicing, are notably elevated in response to HU (Fig. 5E), but not particularly with
25 ETO (Fig. 4E). Interestingly, binding sites for 14-3-3 ϵ , which generally conform to the
26 RXXpS/TXP consensus, were elevated under both conditions, but particularly in response to
27 HU. 14-3-3 proteins are known to be involved in the cellular response to DNA damage; 14-3-
28 3 ϵ in particular, modulates NF- κ B signalling in part by virtue of its ability to bind phosphorylated
29 TAK1 (and its cognate phosphatase PPM1B), and thereby regulate its anti-apoptotic
30 capabilities [66,67]. In response to DNA damage stress, this manifests as inhibition of the anti-
31 apoptotic activity of TAK1, promoting an apoptotic phenotype that is enhanced by the 14-3-
32 3 ϵ -mediated disruption of DP-2 from the E2F transcriptional complex [68]. The fact that we
33 observe elevated putative 14-3-3 ϵ binding sites following HU treatment (but significantly less
34 so with ETO), is in agreement with the pro-apoptotic response of HU-treated cells.
35 Consequently, we hypothesise that the ability of components of the RelA interactome to bind
36 14-3-3 ϵ may be a driving factor in achieving the expected cell death/survival phenotype in
37 response to these two DNA damaging agents.

1 DISCUSSION

2 Protein phosphorylation is a key reversible, dynamic PTM that rapidly governs protein complex
3 formation, particularly of transcription factor complexes, thereby coupling extracellular
4 stressors with compensatory transcriptional output. To understand the role of phosphorylation
5 in regulating the RelA transcriptional network in response to different types of DNA damage,
6 we used a quantitative phosphoproteomics to explore the dynamics of the phosphorylated
7 RelA interactome in response to either ETO or HU. Evaluating the RelA network under these
8 conditions is pertinent, given the central role of this transcription factor in directing the cellular
9 response towards either senescence or apoptosis. Exposure of U2OS cells to either ETO or
10 HU had very limited effect on the phosphorylated RelA interactome; only 246 of the 815 RelA
11 interacting phosphoproteins that we identified in total changed upon treatment. Of these, less
12 than 1% were specific to the type of DNA stress, with 7 or 8 unique proteins (respectively)
13 being identified in the RelA network following exposure of U2OS cells to either the DSB-
14 inducing ETO or to HU. However, although there was little change in the make-up of this
15 network, there was evidence of subtle, but significant, changes in the phosphorylation states
16 of the RelA bound proteins as a function of both the type of and duration of the DNA damaging
17 agent used. Not only did the anti-apoptotic agent ETO invoke a more rapid cellular response
18 than HU, both in terms of maximal H2AX levels (Fig. 1B), and quantifiable changes in
19 phosphopeptide levels (Figs. 3, 4 and 5; Supp. Table 2), but interestingly this study pointed to
20 the differential regulation of key cellular processes and the involvement of unique signalling
21 pathways in modulating the treatment-specific functions of RelA.

22 Examination of the RelA network hub (the bait) revealed two novel phosphorylation events
23 amongst the RelA phosphopeptides that we were able to identify and quantify in this trypsin-
24 based peptide analysis: Thr54 and Ser169, both of which are within the DNA binding domain.
25 However, only Ser45 and Ser131 were statistically differentially regulated in response to either
26 ETO or HU. While Ser131 was statistically elevated upon treatment with ETO at 120 min, the
27 fold change was marginal (1.03-fold), with similar fold change (1.05-fold) being observed for
28 this phosphosite in response to HU, albeit at a shorter 30 min time point. The RelA peptide
29 containing pSer45 was unchanged upon ETO treatment, and was statistically downregulated
30 by 60 min exposure to HU, again with low (1.05) fold change. Given that we were evaluating
31 the total cellular pool of RelA, rather than specifically the nuclear portion where we would
32 expect e.g. Ser45 phosphorylation to have a greater regulatory effect [26], it is perhaps not
33 surprising that the phosphopeptides changes quantified in this study were relatively low.
34 Although a number of our findings of regulated phosphorylation site changes are in agreement
35 with other published studies, the overall fold change in phosphopeptide levels across this
36 study were relatively low (maximally 1.7 fold), and speaks to the necessity to avoid, wherever
37 possible, implementation of a fold-change cut-off during this type of analysis. While ETO-
38 regulated RelA bound phosphoproteins were primarily involved in transcription, cell division

1 and mitosis, and DSB repair (as might be expected), HU-mediated changes were
2 predominantly observed in proteins with functions in rRNA and mRNA processing, and
3 translational initiation. Where changes were observed, ETO predominantly resulted in
4 elevated phosphopeptide levels, with a number of the ETO-regulated phosphorylation sites
5 identified having been reported previously to be modulated in response to either IR or UV
6 radiation. It was interesting to note that transcriptional regulation and DNA damage repair
7 proteins were enriched in those datasets with both elevated and reduced phosphopeptide
8 levels, suggesting coordinated regulation of these processed through different effectors in
9 response to DSB. In addition to the involvement in ATM/ATR signalling previously reported,
10 potential substrates for which were much more prevalent following ETO treatment than HU,
11 kinase substrate prediction suggested roles for CDK1 and ERK1 (or their cognate
12 phosphatases), in regulating RelA complexes in response to ETO. In contrast, levels of the
13 activation loop phosphopeptide in MAPK1/ERK2, traditionally thought to be a marker of kinase
14 activity, were elevated in response to HU, but not ETO, suggesting differential MAPK isoform
15 signalling in response to these two types of DNA damage. The prediction of substrates for
16 p38 α in the regulated phosphorylation sites following cellular exposure to HU (but not ETO),
17 also points to a potential HU-specific regulation of this stress activated protein kinase. Finally
18 our data point to a role for 14-3-3 ϵ binding propensity in facilitating the cellular response to
19 HU, which may be a contributing factor in differentiating the pro-and anti-apoptotic phenotypes
20 that are the result of prolonged cellular expose to these two type of DNA damaging agents,
21 and we believe is worthy of further investigation.

22

23

24

25

26

27

28

29

30

31

32

33

34

35

36

1 **Author Contributions**

2 CEE and NDP obtained funding. AC, CFF and CEE designed the experiments and analysed
3 the data, with bioinformatics support from SP and ARJ. LS generated the HA-RelA U2OS cell
4 line. CFF treated the cells, prepared the samples and did the immunoblotting studies. AC,
5 CFF and PJB performed the MS analysis. AC and CEE wrote the paper with contributions
6 from all authors, who also approved the final version prior to submission.

7

8 **Funding Sources**

9 This work was supported by the Biotechnology and Biological Sciences Research Council
10 (BBSRC; BB/L009501/1 to CEE and NDP, BB/R000182/1 and BB/M012557/1 to CEE) and
11 Cancer Research UK (CRUK; C1443/A22095 to NDP and CEE, and C1443/A12750 to NDP).

12

13 **Notes**

14 The authors declare no competing financial interest. The mass spectrometry proteomics data
15 have been deposited to the ProteomeXchange Consortium via the PRIDE partner repository
16 with the dataset identifiers PXD019587 and PXD019589.

17

18 **Abbreviations**

19 AGC, automatic gain control; CID, collision-induced dissociation; DSB, double strand break;
20 ETD, electron-transfer dissociation; ETcaD, electron transfer with supplemental collision
21 activation; EThcD, electron-transfer higher energy collisional dissociation; ETO, etoposide;
22 GO, gene ontology; HCD, higher energy collisional dissociation; HU, hydroxyurea; IR, ionizing
23 radiation; MS, mass spectrometry; PD, Proteome Discoverer; PTM, post-translational
24 modification; RHD, Rel homology domain; TD, transactivation domain; UV, ultraviolet.

25

26

1 REFERENCES

2 1 Perkins, N. D. (2012) The diverse and complex roles of NF- κ B subunits in cancer.
3 Nat. Rev. Cancer **12**, 121–132.

4 2 Christian, F., Smith, E. and Carmody, R. (2016) The Regulation of NF- κ B Subunits by
5 Phosphorylation. Cells **5**, 12.

6 3 Lu, X. and Yarbrough, W. G. (2015) Negative regulation of RelA phosphorylation:
7 Emerging players and their roles in cancer. Cytokine Growth Factor Rev., Elsevier Ltd
8 **26**, 7–13.

9 4 Giridharan, S. and Srinivasan, M. (2018) Mechanisms of NF- κ B p65 and strategies for
10 therapeutic manipulation. J. Inflamm. Res. **11**, 407–419.

11 5 Kumar, A., Takada, Y., Boriek, A. M. and Aggarwal, B. B. (2004) Nuclear factor- κ B: Its
12 role in health and disease. J. Mol. Med. **82**, 434–448.

13 6 Kim, H. J., Hawke, N. and Baldwin, A. S. (2006) NF- κ B and IKK as therapeutic targets
14 in cancer. Cell Death Differ. **13**, 738–747.

15 7 Didonato, J. A., Mercurio, F. and Karin, M. (2012) NF- κ B and the link between
16 inflammation and cancer. Immunol. Rev. **246**, 379–400.

17 8 Tilstra, J. S., Niedernhofer, L. J., Paul, D., Tilstra, J. S., Robinson, A. R., Wang, J.,
18 Gregg, S. Q., Clauson, C. L., Reay, D. P., Nasto, L. A., et al. (2012) NF- κ B inhibition
19 delays DNA damage – induced senescence and aging in mice Find the latest version :
20 NF- κ B inhibition delays DNA damage – induced senescence and aging in mice **122**,
21 2601–2612.

22 9 Wang, J., Jacob, N. K., Ladner, K. J., Beg, A., Perko, J. D., Tanner, S. M.,
23 Liyanarachchi, S., Fishel, R. and Guttridge, D. C. (2009) RelA/p65 functions to
24 maintain cellular senescence by regulating genomic stability and DNA repair. EMBO
25 Rep., Nature Publishing Group **10**, 1272–1278.

26 10 Chien, Y., Scuoppo, C., Wang, X., Fang, X., Balgley, B., Bolden, J. E., Premsrirut, P.,
27 Luo, W., Chicas, A., Lee, C. S., et al. (2011) Control of the senescence-associated
28 secretory phenotype by NF- κ B promotes senescence and enhances chemosensitivity.
29 Genes Dev. **25**, 2125–2136.

30 11 Slater, M. L. (1973) Effect of reversible inhibition of deoxyribonucleic acid synthesis
31 on the yeast cell cycle. J. Bacteriol. **113**, 263–270.

32 12 Krakoff, I. H., Brown, N. C. and Reichard, P. (1968) Inhibition Reductase of
33 Ribonucleoside by Hydroxyurea1 Diphosphate 1559–1565.

34 13 Stauber, R. H., Knauer, S. K., Habtemichael, N., Bier, C., Unruhe, B., Weisheit, S.,
35 Spange, S., Nonnenmacher, F., Fetz, V., Ginter, T., et al. (2012) A combination of a
36 ribonucleotide reductase inhibitor and histone deacetylase inhibitors downregulates
37 EGFR and triggers BIM-dependent apoptosis in head and neck cancer. Oncotarget **3**,
38 31–43.

1 14 Murai, J. and Pommier, Y. (2019) Phosphatase 1 Nuclear Targeting Subunit, a Novel
2 DNA Repair Partner of PARP1. *Cancer Res.* **79**, 2460–2461.

3 15 Krämer, O. H., Knauer, S. K., Zimmermann, D., Stauber, R. H. and Heinzel, T. (2008)
4 Histone deacetylase inhibitors and hydroxyurea modulate the cell cycle and
5 cooperatively induce apoptosis. *Oncogene* **27**, 732–740.

6 16 Pommier, Y., Leo, E., Zhang, H. and Marchand, C. (2010) DNA topoisomerase and
7 their poisoning by anticancer and antibacterial drugs. *Chem. Biol.*, Elsevier Ltd **17**,
8 421–433.

9 17 Montecucco, A. and Biamonti, G. (2007) Cellular response to etoposide treatment.
10 *Cancer Lett.* **252**, 9–18.

11 18 Montecucco, A., Zanetta, F. and Biamonti, G. (2015) Molecular mechanisms of
12 etoposide. *EXCLI J.* **14**, 95–108.

13 19 Schäfer, C., Göder, A., Beyer, M., Kiweler, N., Mahendarajah, N., Rauch, A.,
14 Nikolova, T., Stojanovic, N., Wieczorek, M., Reich, T. R., et al. (2017) Class I histone
15 deacetylases regulate p53/NF-κB crosstalk in cancer cells. *Cell. Signal.*, Elsevier Inc.
16 **29**, 218–225.

17 20 Schneider, G., Henrich, A., Greiner, G., Wolf, V., Lovas, A., Wieczorek, M., Wagner,
18 T., Reichardt, S., Von Werder, A., Schmid, R. M., et al. (2010) Cross talk between
19 stimulated NF-κB and the tumor suppressor p53. *Oncogene* **29**, 2795–2806.

20 21 Wagner, T., Kiweler, N., Wolff, K., Knauer, S. K., Brandl, A., Hemmerich, P.,
21 Dannenberg, J. H., Heinzel, T., Schneider, G. and Krämer, O. H. (2015) Sumoylation
22 of HDAC2 promotes NF-κB-dependent gene expression. *Oncotarget* **6**, 7123–7135.

23 22 Wu, Z. H. and Miyamoto, S. (2008) Induction of a pro-apoptotic ATM-NF-κB pathway
24 and its repression by ATR in response to replication stress. *EMBO J.* **27**, 1963–1973.

25 23 Perkins, N. D. (2006) Post-translational modifications regulating the activity and
26 function of the nuclear factor kappa B pathway. *Oncogene* **25**, 6717–6730.

27 24 Li, H., Wittwer, T., Weber, A., Schneider, H., Moreno, R., Maine, G. N., Kracht, M.,
28 Schmitz, M. L. and Burstein, E. (2012) Regulation of NF-κB activity by competition
29 between RelA acetylation and ubiquitination. *Oncogene* **31**, 611–623.

30 25 Huang, B., Yang, X. D., Lamb, A. and Chen, L. F. (2010) Posttranslational
31 modifications of NF-κB: Another layer of regulation for NF-κB signalling pathway. *Cell.*
32 *Signal.* **22**, 1282–1290.

33 26 Lanucara, F., Lam, C., Mann, J., Monie, T. P., Colombo, S. A. P., Holman, S. W.,
34 Boyd, J., Dange, M. C., Mann, D. A., White, M. R. H., et al. (2016) Dynamic
35 phosphorylation of RelA on Ser42 and Ser45 in response to TNF a stimulation
36 regulates DNA binding and transcription. *Open Biol.* **6**, 160055.

37 27 Chen, L.-F., Williams, S. A., Mu, Y., Nakano, H., Duerr, J. M., Buckbinder, L. and
38 Greene, W. C. (2005) NF- B RelA Phosphorylation Regulates RelA Acetylation. *Mol.*

1 Cell. Biol. **25**, 7966–7975.

2 28 Nihira, K., Ando, Y., Yamaguchi, T., Kagami, Y., Miki, Y. and Yoshida, K. (2010) Pim-
3 1 controls NF-B signalling by stabilizing RelA/p65. Cell Death Differ. **17**, 689–698.

4 29 Campbell, K. J., Witty, J. M., Rocha, S. and Perkins, N. D. (2006) Cisplatin mimics
5 ARF tumor suppressor regulation of RelA (p65) nuclear factor- κ B transactivation.
6 Cancer Res. **66**, 929–935.

7 30 Msaki, A., Sánchez, A. M., Koh, L. F., Barré, B., Rocha, S., Perkins, N. D. and
8 Johnson, R. F. (2011) The role of RelA (p65) threonine 505 phosphorylation in the
9 regulation of cell growth, survival, and migration. Mol. Biol. Cell **22**, 3032–3040.

10 31 Ferries, S., Perkins, S., Brownridge, P. J., Campbell, A., Eyers, P. A., Jones, A. R.
11 and Eyers, C. E. (2017) Evaluation of Parameters for Confident Phosphorylation Site
12 Localization Using an Orbitrap Fusion Tribrid Mass Spectrometer. J. Proteome Res.
13 **16**, 3448–3459.

14 32 Chawade, A., Alexandersson, E. and Levander, F. (2014) Normalizer: A Tool for
15 Rapid Evaluation of Normalization Methods for Omics Data Sets. J. Proteome Res.
16 **13**, 3114–3120.

17 33 Huber, W., Von Heydebreck, A., Sültmann, H., Poustka, A. and Vingron, M. (2002)
18 Variance stabilization applied to microarray data calibration and to the quantification
19 of differential expression. Bioinformatics **18**.

20 34 Mellacheruvu, D., Wright, Z., Couzens, A. L., Lambert, J. P., St-Denis, N. A., Li, T.,
21 Miteva, Y. V., Hauri, S., Sardiu, M. E., Low, T. Y., et al. (2013) The CRAPome: A
22 contaminant repository for affinity purification-mass spectrometry data. Nat. Methods
23 **10**, 730–736.

24 35 Szklarczyk, D., Gable, A. L., Lyon, D., Junge, A., Wyder, S., Huerta-Cepas, J.,
25 Simonovic, M., Doncheva, N. T., Morris, J. H., Bork, P., et al. (2019) STRING v11:
26 Protein-protein association networks with increased coverage, supporting functional
27 discovery in genome-wide experimental datasets. Nucleic Acids Res. **47**, 607–613.

28 36 Shannon, P., Markiel, A., Ozier, O., Baliga, N. S., Wang, J. T., Ramage, D., Amin, N.,
29 Schwikowski, B. and Ideker, T. (1971) Cytoscape: A Software Environment for
30 Integrated Models. Genome Res. **13**, 426.

31 37 Huang, D. W., Sherman, B. T. and Lempicki, R. A. (2009) Bioinformatics enrichment
32 tools: Paths toward the comprehensive functional analysis of large gene lists. Nucleic
33 Acids Res. **37**, 1–13.

34 38 Huang, D. W., Sherman, B. T. and Lempicki, R. A. (2009) Systematic and integrative
35 analysis of large gene lists using DAVID bioinformatics resources. Nat. Protoc. **4**, 44–
36 57.

37 39 Supek, F., Bošnjak, M., Škunca, N. and Šmuc, T. (2011) Revigo summarizes and
38 visualizes long lists of gene ontology terms. PLoS One **6**.

1 40 Kuznetsova, I., Lugmayr, A., Siira, S. J., Rackham, O. and Filipovska, A. (2019)
2 CirGO: an alternative circular way of visualising gene ontology terms. *BMC*
3 *Bioinformatics, BMC Bioinformatics* **20**, 84.

4 41 Horn, H., Schoof, E. M., Kim, J., Robin, X., Miller, M. L., Diella, F., Palma, A.,
5 Cesareni, G., Jensen, L. J. and Linding, R. (2014) KinomeXplorer: An integrated
6 platform for kinase biology studies. *Nat. Methods, Nature Publishing Group* **11**, 603–
7 604.

8 42 Miller, M. L., Lars Juhl Jensen, Diella, F., Jørgensen, C., Tinti, M., Li, L., Hsiung, M.,
9 Parker, S. A., Bordeaux, J., Sicheritz-Ponten, T., et al. (2008) Linear Motif Atlas for
10 Phosphorylation-Dependent Signalling. *Sci. Signal.* **1**.

11 43 Colaert, N., Helsens, K., Martens, L., Vandekerckhove, J. and Gevaert, K. (2009)
12 Improved visualization of protein consensus sequences by iceLogo. *Nat. Methods,*
13 *Nature Publishing Group* **6**, 786–787.

14 44 Kuo, L. J. and Yang, L. X. (2008) γ-H2AX- A novel biomarker for DNA double-strand
15 breaks. *In Vivo (Brooklyn)*. **22**, 305–310.

16 45 Ward, I. M. and Chen, J. (2001) Histone H2AX Is Phosphorylated in an ATR-
17 dependent Manner in Response to Replication Stress. *J. Biol. Chem.* **276**, 47759–
18 47762.

19 46 Anderson, L. A. and Perkins, N. D. (2003) Regulation of RelA (p65) Function by the
20 Large Subunit of Replication Factor C. *Mol. Cell. Biol.* **23**, 721–732.

21 47 Perkins, N. D., Felzien, L. K., Betts, J. C., Leung, K., Beach, D. H. and Nabel, G. J.
22 (1997) Regulation of NF-κB by cyclin-dependent kinases associated with the p300
23 coactivator. *Science (80-)*. **275**, 523–527.

24 48 Perkins, N. D., Agranoff, A. B., Pascal, E. and Nabel, G. J. (1994) An interaction
25 between the DNA-binding domains of RelA(p65) and Sp1 mediates human
26 immunodeficiency virus gene activation. *Mol. Cell. Biol.* **14**, 6570–6583.

27 49 Girdwood, D., Bumpass, D., Vaughan, O. A., Thain, A., Anderson, L. A., Snowden, A.
28 W., Garcia-Wilson, E., Perkins, N. D. and Hay, R. T. (2003) p300 transcriptional
29 repression is mediated by SUMO modification. *Mol. Cell* **11**, 1043–1054.

30 50 Zhang, B., Wu, J., Cai, Y., Luo, M., Wang, B. and Gu, Y. (2018) AAED1 modulates
31 proliferation and glycolysis in gastric cancer. *Oncol. Rep.* **40**, 1156–1164.

32 51 Matsuoka, S., Ballif, B. A., Smogorzewska, A., McDonald, E. R., Hurov, K. E., Luo, J.,
33 Bakalarski, C. E., Zhao, Z., Solimini, N., Lerenthal, Y., et al. (2007) ATM and ATR
34 substrate analysis reveals extensive protein networks responsive to DNA damage.
35 *Science (80-)*. **316**, 1160–1166.

36 52 Boeing, S., Williamson, L., Encheva, V., Gori, I., Saunders, R. E., Instrell, R., Aygün,
37 O., Rodriguez-Martinez, M., Weems, J. C., Kelly, G. P., et al. (2016) Multiomic
38 Analysis of the UV-Induced DNA Damage Response. *Cell Rep.* **15**, 1597–1610.

1 53 Nicolai, S., Mahen, R., Raschellà, G., Marini, A., Pieraccioli, M., Malewicz, M.,
2 Venkitaraman, A. R. and Melino, G. (2020) ZNF281 is recruited on DNA breaks to
3 facilitate DNA repair by non-homologous end joining. *Oncogene*, Springer US **39**,
4 754–766.

5 54 Enserink, J. M. and Kolodner, R. D. (2010) An overview of Cdk1-controlled targets
6 and processes. *Cell Div.* **5**, 1–41.

7 55 Gonzalez, F. A., Raden, D. L. and Davis, R. J. (1991) Identification of substrate
8 recognition determinants for human ERK1 and ERK2 protein kinases. *J. Biol. Chem.*
9 **266**, 22159–22163.

10 56 Fang, L., Choudhary, S., Zhao, Y., Edeh, C. B., Yang, C., Boldogh, I. and Brasier, A.
11 R. (2014) ATM regulates NF-κB-dependent immediate-early genes via RelA ser 276
12 phosphorylation coupled to CDK9 promoter recruitment. *Nucleic Acids Res.* **42**, 8416–
13 8432.

14 57 Traven, A. and Heierhorst, J. (2005) SQ/TQ cluster domains: Concentrated ATM/ATR
15 kinase phosphorylation site regions in DNA-damage-response proteins. *BioEssays*
16 **27**, 397–407.

17 58 Roskoski, R. (2012) ERK1/2 MAP kinases: Structure, function, and regulation.
18 *Pharmacol. Res.*, Elsevier Ltd **66**, 105–143.

19 59 Cargnello, M. and Roux, P. P. (2011) Activation and Function of the MAPKs and Their
20 Substrates, the MAPK-Activated Protein Kinases. *Microbiol. Mol. Biol. Rev.* **75**, 50–
21 83.

22 60 Wang, Y., Xu, J., Gao, G., Li, J., Huang, H., Jin, H., Zhu, J., Che, X. and Huang, C.
23 (2016) Tumor-suppressor NFκB2 p100 interacts with ERK2 and stabilizes PTEN
24 mRNA via inhibition of MIR-494. *Oncogene* **35**, 4080–4090.

25 61 Gatei, M., Young, D., Cerosaletti, K. M., Desai-Mehta, A., Spring, K., Kozlov, S.,
26 Lavin, M. F., Gatti, R. A., Concannon, P. and Khanna, K. K. (2000) ATM-dependent
27 phosphorylation of nibrin in response to radiation exposure. *Nat. Genet.* **25**, 115–119.

28 62 Wu, X., Ranganathan, V., Weisman, D. S., Heine, W. F., Ciccone, D. N., Neill, T. B.
29 O., Crick, K. E., Pierce, K. A., Lane, W. S., Rathbun, G., et al. (2000) ATM
30 phosphorylation of Nijmegen breakage syndrome protein is required in a DNA
31 damage response. *Nature* **405**, 477–482.

32 63 Tando, T., Ishizaka, A., Watanabe, H., Ito, T., Iida, S., Haraguchi, T., Mizutani, T.,
33 Izumi, T., Isobe, T., Akiyama, T., et al. (2010) Requiem protein links RelB/p52 and the
34 Brm-type SWI/SNF complex in a noncanonical NF-κB pathway. *J. Biol. Chem.* **285**,
35 21951–21960.

36 64 Mulero, M. C., Shahabi, S., Ko, M. S., Schiffer, J. M., Huang, D. Bin, Wang, V. Y. F.,
37 Amaro, R. E., Huxford, T. and Ghosh, G. (2018) Protein Cofactors Are Essential for
38 High-Affinity DNA Binding by the Nuclear Factor κb RelA Subunit. *Biochemistry* **57**,

1 2943–2957.

2 65 Hegde, V., Yadavilli, S. and Deutsch, W. A. (2007) Knockdown of ribosomal protein
3 S3 protects human cells from genotoxic stress. *DNA Repair (Amst.)*. **6**, 94–99.

4 66 Pennington, K., Chan, T., Torres, M. and Andersen, J. (2018) The dynamic and
5 stress-adaptive signalling hub of 14-3-3: emerging mechanisms of regulation and
6 context-dependent protein–protein interactions. *Oncogene*, Springer US **37**, 5587–
7 5604.

8 67 Zuo, S., Xue, Y., Tang, S., Yao, J., Du, R., Yang, P. and Chen, X. (2010) 14-3-3
9 epsilon dynamically interacts with key components of mitogen-activated protein
10 kinase signal module for selective modulation of the TNF- α -Induced time course-
11 dependent NF- κ b activity. *J. Proteome Res.* **9**, 3465–3478.

12 68 Milton, A. H., Khaire, N., Ingram, L., O'Donnell, A. J. and La Thangue, N. B. (2006)
13 14-3-3 Proteins integrate E2F activity with the DNA damage response. *EMBO J.* **25**,
14 1046–1057.

15

